Erschienen in: Optics Letters ; 41 (2016), 2. - S. 246-249
https://dx.doi.org/10.1364/OL.41.000246

615 fs pulses with 17 mJ energy generated by an Yb:thin-disk amplifier at 3 kHz repetition rate

Jonathan Fischer, Alexander-Cornelius Heinrich, Simon Maier, Julian Jungwirth, Daniele Brida, and Alfred Leitenstorfer*

Department of Physics and Center for Applied Photonics, University of Konstanz, D-78457 Konstanz, Germany
**Corresponding author: alfred.leitenstorfer@uni konstanz.de*

A combination of Er/Yb:fiber and Yb:thin-disk technology produces 615 fs pulses at 1030 nm with an average output power of 72 W. The regenerative amplifier allows variation of the repetition rate between 3 and 5 kHz with pulse energies from 13 to 17 mJ. A broadband and intense seed provided by the compact and versatile fiber front-end minimizes gain narrowing. The resulting sub-ps performance is ideal for nonlinear frequency conversion and pulse compression. Operating in the upper branch of a bifurcated pulse train, the system exhibits exceptional noise performance and stability.

OCIS codes: (060.2320) Fiber optics amplifiers and oscillators; (140.3280) Laser amplifiers; (140.7090) Ultrafast lasers; (140.0140) Lasers and laser optics; (320.0320) Ultrafast optics; (140.3460) Lasers.

Ultrashort pulses with energies up to several mJ enable a wide range of applications, from ultrafast science [1,2] to micromachining [3,4]. The traditional technology to generate such output is based on Ti:sapphire. In particular, this broadband gain medium allows for the direct production of intense pulses characterized by a duration of a few tens of femtoseconds. The main limitation of Ti:sapphire is the large quantum defect associated with its absorption band in the green spectral region, necessitating elaborate strategies for thermal management and application of relatively sophisticated pump lasers. In fact, cryocooling of the gain rod is required already at a level of 15 W of output power. Ytterbium doped media are becoming increasingly popular to overcome thermal issues and to obtain high intensity output [5,6]. In fact, due to minimum quantum defect and direct diode pumping in the near infrared, Yb doped fibers [7,8] and thin disks [2,3,9–17] combine power scalability [14] with maximum flexibility in the repetition rate. Ultrafast Yb:thin disk [3] lasers are particularly appealing for the generation of mJ level pulses and high average power [15] due to the efficient heat extraction [17] from the thin gain medium.

In this Letter, we exploit the benefits of Yb:thin disks in a regenerative amplifier that operates at average output powers exceeding 70 W. In addition, we tackle the bandwidth limitation of Yb:YAG using a seed source that combines the robustness and flexibility of femtosecond Er:fiber technology with the efficiency of Yb:fiber amplifiers. The broadband and intense input allows us to limit gain narrowing and to achieve sub ps pulse duration in the regenerative amplifier. The pulses are still more than 10 times longer as compared to what may be achieved with Ti:sapphire systems, but already short enough to drive key nonlinear processes such as white light generation in dielectrics. This fact enables efficient implementation of front end ultrafast sources, such as optical parametric amplifiers (OPAs), for the generation of ultrabroadband, ultraintense, and widely tunable output.

Figure 1 outlines the setup of the system. The seed laser starts with an Er:fiber oscillator followed by a preamplifier stage [18]. The repetition rate is then reduced from the native 40 to 10 MHz by an electro optic modulator. The following femtosecond Er:amplifier produces 100 fs pulses with an energy of 10 nJ after a Si prism sequence. A highly nonlinear fiber (HNF) converts the output from 1550 nm to the Yb gain bandwidth centered at a wavelength of 1030 nm [18,19].

The resulting spectrum is shown as a dashed green line in the inset of Fig. 2(a). It contains 700 μW of average power. The full width at half maximum (FWHM) spectral bandwidth of 68 nm covers the entire Yb fiber gain window. The seed [8] is stretched in a grating pair with approximately 105 ps^2 of group delay dispersion [20], resulting in a 2 ns (FWHM) output for linear chirped pulse amplification. This signal is amplified to a pulse energy of 100 nJ in a 1.2 m long Yb:fiber. The resulting average power of 1 W corresponds to a gain of 31.5 dB. This Yb preamplifier is operated in a deeply saturated regime [see Fig. 2(a)] and provides a pulse train with exceptional stability [8]. The Yb:fiber output exhibits a FWHM spectral bandwidth of 13 nm [Fig. 2(b)]. It is adjusted to provide optimal seed conditions for the Yb:YAG thin disk. The spectral shape results from the gain profile of the Yb:fiber combined with the transmission characteristics of the grating stretcher.

All fiber components are purely single mode and polarization maintaining to warrant an optimum transverse beam profile and defined polarization state as required for efficient amplification with the thin disk. Due to the stretching of the signal to 2 ns,

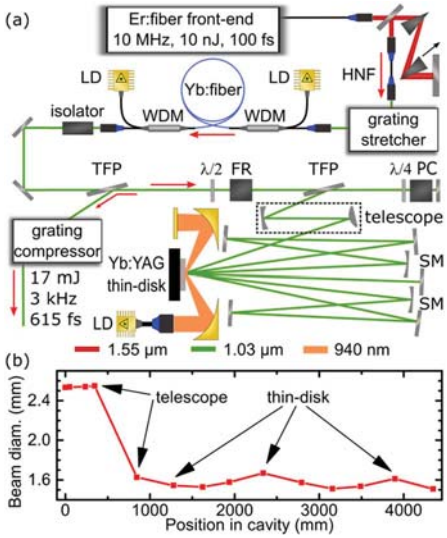

Fig. 1. (a) Setup of the Yb:YAG thin disk regenerative amplifier system. The Er:fiber front end consists of a 40 MHz oscillator and 10 MHz preamplifier. Frequency shift to 1030 nm occurs in a highly nonlinear fiber (HNF). The Yb:fiber preamplifier is pumped bi directionally by wavelength stabilized laser diodes (LD) coupled by wavelength division multiplexers (WDM). Seed injection and extrac tion in the regenerative amplifier cavity is obtained by a combination of thin film polarizers (TFP), waveplates ($\lambda/2$), a Faraday rotator (FR), and a 7 mm clear aperture BBO Pockels cell (PC). A telescope inside the amplifier cavity regulates the spot size at Pockels cell and thin disk for reduced peak intensity and for mode matching between pump and signal beams, respectively. Two spherical mirrors (SM) ensure stable operation of the resonator. (b) Calculated beam spot size (FWHM of the intensity) during propagation inside the regenerative cavity.

no accumulation of nonlinear phase is noticeable in the Yb:fiber system. To avoid destructive feedback between amplifiers, all stages are separated by optical isolators.

The regenerative amplifier employs a Yb:YAG thin disk provided by TRUMPF Laser GmbH as gain medium. The 10 mm diameter disk has a thickness of ~100 μm, a doping level of approximately 10% to 15%, and a radius of curvature of ~20 m. It is thermally back contacted to a water cooled dia mond heat sink. The medium is continuously pumped at a wavelength of 940 nm by a stack of fiber coupled laser diodes. We obtain a Gaussian inversion profile of 2 mm diameter (FWHM). The repetition rate of the regenerative thin disk am plifier is controlled via a 20 mm long BBO Pockels with an aperture of 7 mm, as sketched in Fig. 1. An all reflective tele scope is implemented into the cavity to keep the peak intensity below the damage threshold of the Pockels cell. Optimum mode matching is achieved at the gain medium, resulting in efficient energy extraction. The regenerative cavity is designed with a folded path so that the disk is exploited six times per roundtrip. Two spherical mirrors add focusing power to meet the conditions for a stable resonator. The B integral is kept well below 1, ensuring negligible nonlinear broadening or phase modulation. Figure 1(b) shows the evolution of the spot size along the cavity. The overall optical path in the regenerative amplifier amounts to 9 m, corresponding to an equivalent repetition rate of 33 MHz. The angle of incidence of the beam path is kept below 5° with respect to the surface normal to min

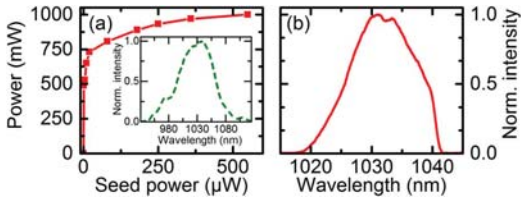

Fig. 2. (a) Output power of the Yb:fiber preamplifier as a function of seed power. Inset: input spectrum to the Yb:fiber preamplifier, as measured after the HNF. (b) Output spectrum of the Yb:preamplifier.

imize aberrations. After 20 complete roundtrips, corresponding to 120 passes through the disk and a total amplification cycle of 0.6 μs, a gain in energy as large as 60 dB is obtained, and 20 mJ pulses are produced at a 3 kHz repetition rate. An aver age output power of 72 W is achieved under 172 W of CW pumping at a wavelength of 940 nm, corresponding to an optical to optical efficiency of 42%. The spectrum of the amplifier pulse train is depicted in Fig. 3(a). It supports a transform limited pulse duration of 580 fs. The bandwidth of 2 nm around the central wavelength of 1030 nm emerges due to gain narrowing. A slope efficiency as high as 48% is evident from Fig. 3(b). Our thin disk system works under ambient atmosphere and avoids cryogenic cooling [21]. The amplifier cavity generates the high quality TEM_{00} mode shown in Fig. 3(c) with $M^2 = 1.5$. In addition, the linear polarization of the seed is fully preserved.

It should be noted that the thin disk amplifier operates in a bifurcated regime [11,22,23], i.e., it generates two equidistant trains of pulses with alternating energy content at half the rep etition rate set by the Pockels cell. In fact, for obtaining a pulse train at 3 and 5 kHz repetition rates, the Pockels cell is driven at 6 and 10 kHz, respectively. Such bifurcation phenomena occur in systems where the inverse upper state lifetime of the active medium (Yb:YAG: $\tau_{up} = 1$ 2 ms at room temperature [24]) is in the range of the inverse repetition rate, and the pulse energy is high enough to cause substantial depletion of the inverted medium. Due to the nonlinear character of the gain dynamics, subsequent seed pulses encounter two distinct inver

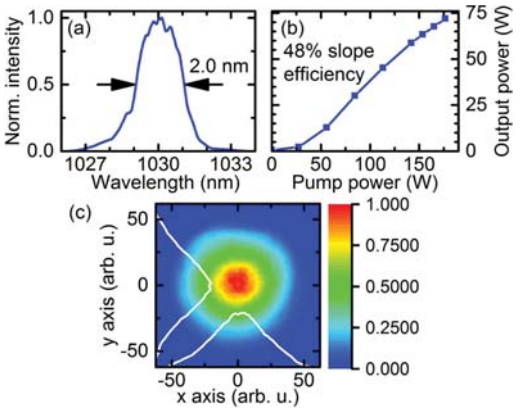

Fig. 3. (a) Yb:thin disk output spectrum at 72 W of average power. (b) Average power of the regenerative thin disk amplifier as a function of pump power. The slope efficiency is 48%. The maximum pulse energy at 3 kHz repetition rate amounts to 20 mJ. (c) Normalized transverse intensity profile (color coded) of amplifier after grating com pressor at full power with cuts across the center (white solid lines).

sion levels of the active medium. Under these conditions, the average output depends continuously on the pump power [Fig. 4(a)], while the pulse energy may split after several round trips. This behavior is studied experimentally for intermediate pumping levels [solid lines in Fig. 4(b)] while, at the maximum pump power of 172 W, no variations were carried out to avoid damage [black squares in Figs. 4(a) and 4(b)]. A small number of roundtrips at elevated excitation power causes inefficient gain depletion which may result in destructive heat deposition in the thin disk. Therefore, the gain dynamics has been simu lated for some pump levels [dashed lines in Fig. 4(b)] by solving a set of coupled rate equations [22], adopting a saturation en ergy of 1 J, small signal gain of 24% (corresponding to around 3% of single pass amplification), cavity losses of 3%, and a seed pulse energy of 100 nJ. All values of repetition rates and pulse energies reported in the previous sections refer exclusively to the more intense branch after bifurcation. The typical splitting ratio that we obtain when driving the Pockels cell at 6 kHz is 6∶1 so that 72 W of total output result in a 3 kHz main pulse train of 60 W and 12 W is lost in the secondary train. Seeding at 10 kHz, the ratio is 12∶1 with the 5 kHz intense train con taining 65 W of average power.

The amplifier works in the center of the first bifurcated branch to obtain maximum pulse energy while maintaining controllable and stable operation conditions. The system dis plays excellent noise performances since it is operated far from additional bifurcations that would occur at even higher pump ing levels. Recording the energy of each output pulse with a boxcar detection scheme, we obtain relative root mean square fluctuations of 7.0×10^{-3} over a time window of 20 min [Fig. 4(c)]. This measurement was taken with the laser in a free running mode without any active stabilization scheme.

The amplified pulse train is compressed by a pair of multi layer dielectric gratings [25,26] (line density of 1760 l/mm) with a separation of 80 cm. Nearly transform limited perfor mance is achieved by careful design of the stretcher/compressor combination. To characterize the pulse after compression, we retrieve second harmonic generation frequency resolved optical gating (SHG FROG) [27] at full output power.

Figure 5(a) shows the measured FROG data, whereas Fig. 5(b) presents the reconstructed trace. The retrieved tem poral intensity profile and phase is depicted in Fig. 5(c), yielding a FWHM pulse duration of 615 fs. The spectral in tensity profile and phase are found in Fig. 5(d). The diffraction efficiency of each dielectric grating is higher than 95%, ensur ing an overall throughput of 82%. A compressed pulse energy of 17 mJ results when the system operates at 3 kHz, while 13 mJ are obtained at an effective repetition rate of 5 kHz.

While it is straightforward to obtain single filament white light supercontinua (WLC) with intense pulses of a duration of hundreds of femtoseconds, this task becomes increasingly chal lenging when the driving pulse exceeds one picosecond [28]. The pulses produced by our Yb:thin disk amplifier are short enough to allow for the direct generation of WLC in a thin dielectric plate. Efficient generation of a stable WLC underlines the favorable noise performance of the laser system, proper pulse compression, and gentle behavior of the phase. For the WL generation, we spilled a pulse train with energies below 10 μJ from the fundamental beam. Focusing with a 125 mm lens into a 5 mm thick YAG plate, we observe a significant spectral broadening when exceeding 2 μJ of driving energy. The peak intensity is 6 GW/cm^2 at a spot size of 70 μm. The resulting WLC spans a wavelength of 500 to 1300 nm. Pulse to pulse intensity fluctuations are smaller than 0.75%. A typical spectrum is depicted in Fig. 6.

In conclusion, we introduce an Yb:YAG thin disk amplifier seeded by a combination of a compact and versatile femtosec ond Er:fiber system with a core pumped Yb:fiber preamplifier. The output pulses reach up to 17 mJ energy, with a duration of 615 fs at a repetition rate of 3 kHz and a wavelength of 1030 nm. Featuring a peak power above 28 GW as calculated from the measured pulse envelope and energy, this tabletop sys tem with a footprint of 1 m^2 represents an ideal driving source for advanced experiments requiring high stability and pulse

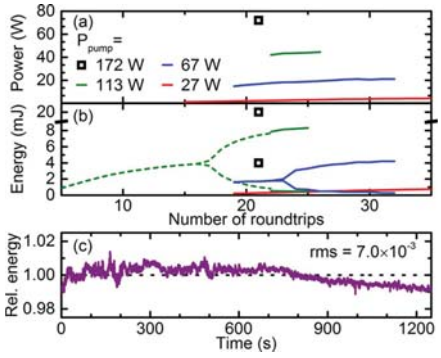

Fig. 4. (a) Uncompressed output power of the combined high and low energy pulse trains produced by the thin disk amplifier as a func tion of the number of roundtrips for different pump power levels P_{pump}. (b) Pulse energy as a function of the number of roundtrips. The repetition rate is 6 kHz before bifurcation and 3 kHz for each branch afterward, respectively. No bifurcation is observed below 27 W of pump power. Increasing P_{pump} results in an earlier onset of bifur cation. Solid lines depict experimental data, while dashed lines result from a simulation of the nonlinear amplification dynamics. The opera tional point for the highest available pump power is indicated by black squares, respectively. (c) Relative pulse energy as a function of time with the amplifier system operating at a 5 kHz repetition rate and 60 W of average output power.

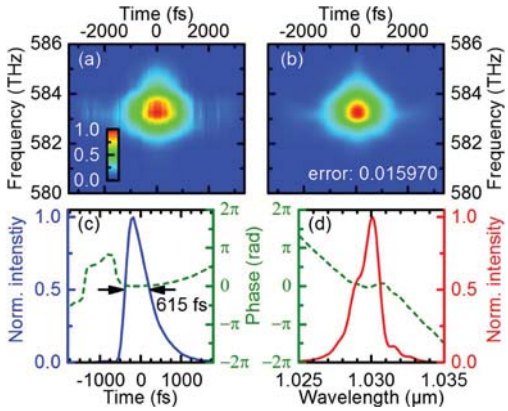

Fig. 5. SHG FROG of compressed 17 mJ pulses. (a) Amplitude of measured FROG trace (128 × 128 pixels grid). (b) Retrieved FROG trace in amplitude with reconstruction pixel error of 0.015970. (c) Temporal intensity (solid blue line) and phase (dashed green line). (d) Spectral intensity (solid red line) and phase (dashed green line). The pulse duration is 615 fs, while the Fourier limit of the retrieved spectrum amounts to 560 fs.

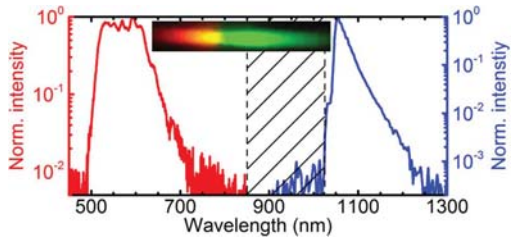

Fig. 6. Spectrum of the white light supercontinuum generated in a 5 mm thick YAG plate. A broad maximum in the visible domain starts around a wavelength of 500 nm and extends up to 750 nm. The infra red part can be tuned to reach up to 1300 nm. The spectra are sep arately normalized. The blind stitched region was blocked by color filters to minimize the contribution of the fundamental pump pulse at 1030 nm wavelength. The inset shows a photograph of the visible part of the white light as dispersed by a fused silica prism.

energy at the same time. Intensities as high as 500 PW/cm^2 under diffraction limited focusing suggest applications in ex treme nonlinear optics. In addition, we demonstrate stable white light generation that constitutes an important milestone for the direct application of the laser system as a pump source for nonlinear frequency conversion and ultrashort pulse com pression based, for example, on OPAs. This approach will allow for the generation of ultrabroadband and ultraintense pulses tunable from the near to far infrared spectral range [29 32]. Other appealing applications exploit the flexibility of the seed source and its capability of producing intrinsically synchronized and passively phase stable few cycle pulses via parallel ampli fiers [18]. In fact, one of the four synchronized seed laser arms is equipped with an Er:fiber amplifier and HNF to generate 500 nm broad spectra that are compressed to a duration shorter than 10 fs [19]. This output is readily available, e.g., for sensi tive electro optic sampling [33] or as an alternative seed source for OPAs or chirped pulse OPAs that are able to deliver intense pulses with a duration approaching a single optical cycle [31].

Funding. European Research Council (ERC) (290876); Deutsche Forschungsgemeinschaft (DFG) (INST 38/509 1).

Acknowledgment. The authors thank Dominik Bauer, Thomas Dekorsy, and Dirk Sutter for valuable discussions. Efficient support has been provided by TRUMPF Laser GmbH.

REFERENCES

1. T. Brabec and F. Krausz, Rev. Mod. Phys. **72**, 545 (2000).
2. H. Fattahi, H. G. Barros, M. Gorjan, T. Nubbermeyer, B. Alsaif, C. Y. Yeisset, M. Schultze, S. Prinz, M. Haefner, M. Ueffing, A. Alismail, L. Vamos, A. Schwarz, O. Pronin, J. Bons, X. T. Geng, G. Arisholm, M. Ciappina, V. S. Yakovlev, D. E. Kim, A. M. Azzeer, N. Karpowicz, D. Sutter, Z. Major, T. Metzger, and F. Krausz, Optica **1**, 45 (2014).
3. S. Nolte, F. Schrempel, and F. Dausinger, eds., *Ultrashort Pulse Laser Technology Laser Sources and Applications*, Springer Series in Optical Sciences 195 (Springer, 2016).
4. B. N. Chichkov, C. Momma, S. Nolte, F. von Alvensleben, and A. Tünnermann, Appl. Phys. A **63**, 109 (1996).
5. L. D. DeLoach, S. A. Payne, L. L. Chase, L. K. Smith, W. L. Kway, and W. F. Krupke, IEEE J. Quantum Electron. **29**, 1179 (1993).
6. W. F. Krupke, IEEE J. Quantum Electron. **6**, 1287 (2000).
7. C. Jauregui, J. Limpert, and A. Tünnermann, Nat. Photonics **7**, 861 (2000).
8. M. Wunram, P. Storz, D. Brida, and A. Leitenstorfer, Opt. Lett. **40**, 823 (2015).
9. C. R. E. Baer, C. Kränkel, C. J. Saraceno, O. H. Heckl, M. Golling, R. Peters, K. Petermann, T. Südmeyer, G. Huber, and U. Keller, Opt. Lett. **35**, 2302 (2010).
10. D. Bauer, I. Zawischa, D. H. Sutter, A. Killi, and T. Dekorsy, Opt. Express **20**, 9698 (2012).
11. T. Metzger, A. Schwarz, C. Y. Teisset, D. Sutter, A. Killi, R. Kienberger, and F. Krausz, Opt. Lett. **34**, 2123 (2009).
12. C. J. Saraceno, F. Emaury, C. Schriber, A. Diebold, M. Hoffmann, M. Golling, T. Südmeyer, and U. Keller, IEEE J. Sel. Top. Quantum Electron. **21**, 106 (2015).
13. J. Brons, V. Pervak, E. Fedulova, M. Seidel, D. Bauer, D. Sutter, V. Kalashnikov, A. Apolonski, O. Pronin, and F. Krausz, Opt. Lett. **39**, 6442 (2014).
14. A. Giesen and J. Speiser, IEEE J. Quantum Electron. **13**, 598 (2007).
15. J. P. Negel, A. Loescher, A. Voss, D. Bauer, D. Sutter, A. Killi, M. A. Ahmed, and T. Graf, Opt. Express **23**, 21064 (2015).
16. J. T. Green, J. Novák, R. Antipenkov, F. Batysta, C. Zervos, J. A. Naylon, T. Mazanec, M. Horáček, P. Bakule, and B. Rus, Proc. SPIE **9342**, 93420T (2015).
17. A. Giesen, H. Hügel, A. Voss, K. Wittig, U. Brauch, and H. Opower, Appl. Phys. B **58**, 365 (1994).
18. D. Brida, G. Krauss, A. Sell, and A. Leitenstorfer, Laser Photon. Rev. **8**, 409 (2014).
19. A. Sell, G. Krauss, R. Scheu, R. Huber, and A. Leitenstorfer, Opt. Express **17**, 1070 (2009).
20. O. E. Martinez, J. Opt. Soc. Am. B **3**, 929 (1986).
21. A. Pugzlys, G. Andriukaitis, A. Baltuska, L. Su, J. Xu, H. Li, R. Li, W. J. Lai, P. B. Phua, A. Marcinkevicius, M. E. Fermann, L. Giniunas, R. A. Danielius, and S. Alisauskaus, Opt. Lett. **34**, 2075 (2009).
22. J. Dörring, A. Killi, U. Morgner, A. Lang, M. Lederer, and D. Kopf, Opt. Express **12**, 1759 (2004).
23. M. Grishin and A. Michailovas, *Advances in Solid State Lasers* (INTECH, 2010), p. 630.
24. J. Dong, M. Bass, Y. Mao, P. Deng, and F. Gan, J. Opt. Soc. Am. B **20**, 1975 (2003).
25. M. D. Perry, R. D. Boyd, J. A. Britten, D. Decker, B. W. Shore, C. Shannon, and E. Shults, Opt. Lett. **20**, 940 (1995).
26. J. Neauport, E. Lavastra, G. Raze, G. Dupuy, N. Bonod, M. Balas, G. de Villele, J. Flamand, S. Kaladgew, and F. Desserouer, Opt. Express **15**, 12508 (2007).
27. R. Trebino, K. W. DeLong, D. N. Fittinghoff, J. N. Sweetser, M. A. Krumbügel, B. A. Richman, and D. J. Kane, Rev. Sci. Instrum. **68**, 3277 (1997).
28. A. L. Calendron, H. Çankaya, G. Cirmi, and F. X. Kärtner, Opt. Express **23**, 13866 (2015).
29. B. Mayer, C. Schmidt, J. Bühler, D. V. Seletskiy, D. Brida, A. Pashkin, and A. Leitenstorfer, New J. Phys. **16**, 063033 (2014).
30. S. Witte and K. S. E. Eikema, IEEE J. Quantum Electron. **18**, 296 (2012).
31. S. W. Huang, G. Cirmi, J. Moses, K. H. Hong, S. Bhardwaj, J. R. Birge, L. J. Chen, E. Li, B. J. Eggleton, J. Cerullo, and F. X. Kärtner, Nat. Photonics **5**, 475 (2011).
32. D. Brida, G. Cirmi, C. Manzoni, S. Bonora, P. Villoresi, S. De Silvestri, and G. Cerullo, Opt. Lett. **33**, 741 (2008).
33. C. Kübler, R. Huber, and A. Leitenstorfer, Semicond. Sci. Technol. **20**, S128 (2005).